Available online at www.sciencedirect.com
ScienceDirect
Scripta Materialia 58 (2008) 45–48
Scripta MATERIALIA
www.elsevier.com/locate/scriptamat

Photoabsorption characterization and magnetic property of multiferroic $BiFeO_3$ nanotubes synthesized by a facile sol–gel template process

Jie Wei, Desheng Xue* and Yan Xu

Key Laboratory for Magnetism and Magnetic Materials of MOE, Lanzhou University, Lanzhou 730000, Gansu Province, China

Received 16 May 2007; revised 4 August 2007; accepted 2 September 2007

This paper reports the synthesis and characterization of multiferroic $BiFeO_3$ nanotubes. Perovskite $BiFeO_3$ nanotubes with outer diameters 150–190 nm were synthesized by a facile sol–gel template method. The photoabsorption of $BiFeO_3$ nanotubes was characterized by UV–visible diffuse reflectance spectrometry. The $BiFeO_3$ nanotubes show weak ferromagnetism at room temperature, unlike the antiferromagnetic order in bulk $BiFeO_3$, reflecting the grain size-confinement effect on the magnetic ordering of $BiFeO_3$.

Keywords: Nanotube; Sol–gel; Perovskites; Magnetic properties; Optical properties

Multiferroic materials, which are simultaneously ferroelectric, ferromagnetic and ferroelastic in the same material, have a wide range of potential applications in information storage, spintronic devices and sensors. Of all the multiferroics, $BiFeO_3$ (BFO), in which ferroelectric and antiferromagnetic order coexist, has been the subject of much interest due to its relatively high Néel temperature ($T_N \sim 375$ °C) and Curie temperature ($T_C \sim 830$ °C) [1,2], which make it one of the prime candidates for room-temperature magnetoelectric (ME) applications. However, superimposed on BFO's antiferromagnetic order, there is a spiral spin structure in which the antiferromagnetic axis rotates through the crystal with an incommensurate long-wavelength period of 62 nm [3]. This spiral spin structure cancels the macroscopic magnetization and also inhibits the observation of the linear ME effect in bulk BFO [4].

Recent approaches have focused on developing oriented, epitaxial thin films of BFO grown on a range of substrates including Si, $SrTiO_3$, $SrRuO_3$, $LaNiO_3$, Pt/Ti/SiO_2/Si and Pt/TiO_2/SiO_2/Si [5–11]. However, a fundamental understanding of the structure–property correlations in BFO—specifically, the nature of the magnetic response and the fundamental dependence of magnetic behavior on sample size—are still lacking. Ordered BFO nanotube arrays are very interesting not only for future applications such as vertical magnetic recording media, but their controllable size also enables the intrinsic magnetic properties of BFO to be studied. Furthermore, Bi-containing oxides often offer interesting optical properties for photocatalytic applications [12–14], and it would therefore be attractive to explore the possibilities of using BFO nanotubes as photocatalysts.

Oxide nanotubes are generally prepared by a traditional sol–gel template process, in which the templates are usually dipped into the relevant sols directly; the only driving force of this technique is capillary action. Therefore, filling the pores is difficult, especially for small-pore diameter templates. In recent years, sol–gel electrophoresis deposition has been developed to fabricate one-dimensional nanostructures [15]. However, this process is usually very complex and requires special equipment. In this paper, BFO nanotube arrays were successfully prepared by a facile sol–gel template method that overcame the above-mentioned limitations to a certain extent. At the same time, the photoabsorption of BFO nanotubes was characterized and their magnetic properties investigated.

The porous nanochannel alumina (NCA) templates used in this work were prepared by anodization [16,17]. The BFO sol–gel precursor was prepared as follows: bismuth nitrate $Bi(NO_3)_3 \cdot 5H_2O$ and iron nitrate $Fe(NO_3)_3 \cdot 9H_2O$ were initially dissolved in relatively dilute nitric acid to form a transparent solution. Citric

* Corresponding author. Tel./fax: +86 931 8912726; e-mail: xueds@lzu.edu.cn

1359-6462/$ - see front matter © 2007 Published by Elsevier Ltd. on behalf of Acta Materialia Inc.
doi:10.1016/j.scriptamat.2007.09.001

acid and deionized water were added to the above solution and the concentration of the final solution adjusted to 0.01 M. The pH value of the final solution was adjusted to near neutral using ammonia, and then urea was added to the solution; the molar ratio of cations and urea was 1:20. The NCA templates were put into a vessel which contained an appropriate amount of the above-mentioned solution. The temperature of the vessel was kept at 80 °C for 20 h. In order to obtain the perovskite BFO nanotubes, the filled templates were heat treated in air at 650 °C for 5 h.

The structure and morphology of the BFO nanotubes were examined by X-ray diffraction (XRD), scanning electron microscopy (SEM) and transmission electron microscopy (TEM). Thermogravimetric analysis (TGA) and differential thermal analysis (DTA) were carried out over the temperature range 500–900 °C in nitrogen ambient to study the ferroelectric phase transitions. The UV–visible diffuse reflectance spectrum of the BFO nanotubes was measured by UV–visible spectrometry. A vibrating sample magnetometer (VSM) was used to measure the magnetic properties of BFO nanotubes. In order to carry out the TEM, TGA/DTA, photoabsorption characterization and magnetic properties measurement of BFO nanotubes, the prepared samples were immersed in a 2 M NaOH solution for 36 h to free the BFO nanotubes. The final products were collected and washed thoroughly with deionized water.

In this current work we have improved the urea-nitrate sol–gel template process detailed in Ref. [18], and successfully prepared the multicomponent oxide nanotubes by adding the chelating agent, citric acid. Here, we briefly describe the possible formation process of BFO nanotubes. In our experiments, citric acid was used as chelating agent to form a metal–citrate complex which could stabilize in the aqueous solution. When the solution was heated, the pH value of the solution increased to ~8.0 because urea undergoes hydrolysis above 60 °C as follows:

$$(NH_2)_2CO + 3H_2O \rightarrow 2NH_4^+ + 2OH^- + CO_2$$

The OH^- ions then combined with the metal–citrate complex to form negatively charged sol particles. Meanwhile, the pore walls of the NCA templates were positively charged [19]. Therefore, the sol particles can easily fill the pores of the templates due to electrostatic attraction. The density of sol particles was larger near the wall of pores, and it is reasonable to assume that the nanotubes first formed near the wall areas of the pores and then gradually extended to the center area. During the annealing process, the sol within the NCA nanochannels would be changed into gel by the condensation reactions, and the gel was further turned into BFO nanotubes.

Figure 1a shows a top view SEM image of BFO nanotube arrays grown within the NCA templates. It can be seen that almost all pores of the NCA template are filled with the BFO nanotubes. The inset of Figure 1a is a high-magnification SEM image showing clearly the morphology of the vertical BFO nanotube arrays; the outer diameter of these nanotubes is about 150–190 nm. All of the reflections in the XRD pattern of

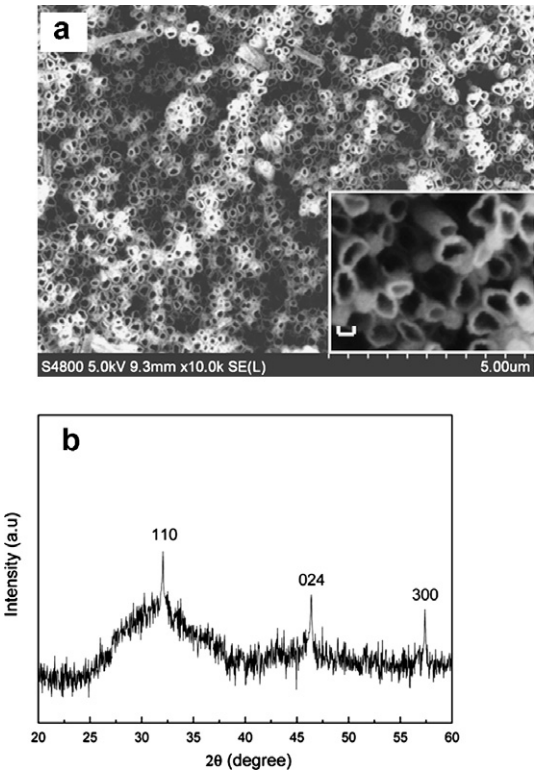

Figure 1. (a) SEM image of BFO nanotube arrays; inset shows a close up of vertical BFO nanotube arrays (bar = 100 nm). (b) XRD pattern of the BFO nanotubes within the NCA templates.

BFO nanotubes within the NCA templates shown in Figure 1b can be indexed as a perovskite BFO structure. No observable second phases were detected.

Figure 2a shows a typical TEM image of BFO nanotubes after alumina was dissolved away. It can be seen that they are apparently tubular in character with a uniform diameter. Figure 2b shows a TEM image of a single BFO nanotube with an outer diameter of about 180 nm. The thickness of wall is estimated to be about 20 nm. The inset of Figure 2b shows the selected area electron diffraction (SAED) pattern taken from the BFO nanotube, which reveals the polycrystalline structure nature of the BFO nanotubes.

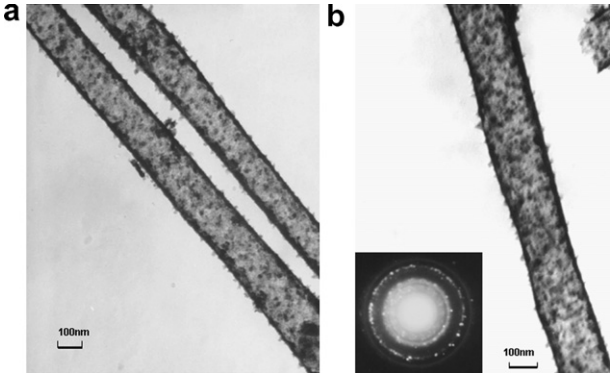

Figure 2. (a) TEM image of BFO nanotubes after dissolving away the NCA templates. (b) TEM image of an isolated BFO nanotube showing the SAED pattern.